



*Thayer School
of Engineering*
at Dartmouth College

Fermentation Modeling Cellulosic Biomass Conversion

ISMIP 5
5th International Symposium
on Mixing in Industrial Processes
Seville, Spain, June 1-4, 2004

André Bakker (Presenter)
Fluent Inc.

Charles E. Wyman, Lee R. Lynd, Jonathan Mielenz
Dartmouth College

Welcome. Today I will speak about the modeling of fermentations involving the conversion of cellulosic biomass to ethanol. This is a multistage fermentation process that involves both aerobic, multiphase fermentations, and anaerobic multi-species fermentations. The modeling work is a cooperation between Fluent Inc, and the Thayer School of Engineering at Dartmouth College in Hanover, NH, just down the road from us. My collaborators are profs. Charlie Wyman, Lee Lynd, and Jonathan Mielenz, all from Dartmouth College.

Introduction

- Dartmouth College Biocommodity Research Initiative.
- Objectives:
 - Develop efficient processes to convert lignocellulosic biomass into ethanol.
 - Ethanol to be used as a transportation fuel:
 - About 2/3 of petroleum goes to transportation.
 - Transportation is almost totally dependent on petroleum (>96%).
 - Biomass can either be waste or specially grown.
- US government invests in this research.
- Current project is a cooperation between the Thayer School of Engineering at Dartmouth College and Fluent Inc.
- Funding acknowledgment: National Institute of Standards and Technology (NIST).



*Thayer School
of Engineering
at Dartmouth College*

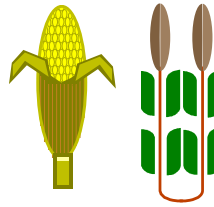
This project is part of a long-term research program called the Dartmouth College Biocommodity Research Initiative. The research involves the conversion of lignocellulosic biomass into ethanol. The objectives of this research are to develop efficient processes to convert the biomass into ethanol. This biomass will usually consist of biologically grown fibrous materials that contain a mixture of cellulose, lignin, and hemicellulose. Cellulose is essentially a polymer of glucose (sugar) molecules that can be broken down into individual glucose molecules. The resulting glucose can then be converted into ethanol through a yeast fermentation. The ethanol can be used as a transportation fuel, either by itself or as an additive to diesel or gasoline (petrol for the Europeans). The biomass to be converted can either be leftover waste from other processes, or it can be specially grown for this purpose. The objective of the research is to reduce the need for petroleum (oil) based fuels. Right now about 2/3 of all petroleum is used for transportation. That sector is almost completely dependent on petroleum (96%) and because of the lack of a backup energy source would be very hard-hit if there were disruptions in the oil supply. The US government is therefore very interested in research into alternative fuel sources for transportation. It is subsidizing such research through a number of channels. The current project is funded by the National Institute of Standards and Technology (NIST). NIST is funding this large-scale biocommodity research program at Dartmouth College. Most of this involves experimental and analytical modeling studies, and in addition CFD work. The CFD work, as said, is a cooperation between DMC and Fluent.

Biomass-ethanol conversion

- **Benefits:**
 - Ethanol fuel has little, if any net carbon dioxide emissions.
 - Solid waste disposal.
 - Low impact biomass crops.
 - Abundant, low-cost feedstock.
 - Sustainable resource supply.
- **Bottlenecks:**
 - Cost of overcoming the recalcitrance of cellulosic biomass.
 - Most costly process steps.
 - Technically immature process.
 - Enzyme, microbial processes have outstanding potential.



Switchgrass



Cellulose 43-45%
Hemicellulose 25-30%
Lignin 15-22%

*Thayer School
of Engineering
at Dartmouth College*



So, what are the benefits of this biomass to ethanol conversion process and the use of ethanol as a transportation fuel.

Let's first look at what we need (see pictures on right). We need something that can be converted to sugar. Most biological materials contain cellulose (in the 43-45% range), hemicellulose (25-30% range) and lignin (in the 15-22% range). All of those are saccharides. Cellulose consists of long polymeric glucose chains. Hemicellulose is also a saccharide, but instead of long polymeric chains it has an amorphous structure. Lignin also consists of polymeric glucose chains but with different chemical bonds than cellulose and is much harder to break down. Sources of biomass, also sometimes called lignocellulosic biomass (because of the lignin and cellulose content), can be existing agricultural waste, or specially grown plants. Specially grown plants can be herbaceous crops, fast growing trees such as poplar trees that are harvested every six to eight years, or simple plants such as the switchgrass shown here.

Compared to using gasoline as a fuel, ethanol has many environmental benefits, such as little or no net carbon dioxide emissions. The biomass grown takes up approximately the same amount of CO₂ out of the atmosphere as is being produced when it is combusted in an engine. It also allows for the disposal of large amounts of solid waste that are currently being dumped into landfills. When using specially grown biomass sources, one can cultivate crops that have both low-environmental impact (low water requirements and low erosion) and a high net energy content. From an economic perspective it is attractive because of a number of reasons. These include the fact that biomass is available in abundance and can be considered a sustainable resource supply.

Some of the practical bottlenecks in this conversion process are the cost of overcoming the recalcitrance of cellulosic biomass to such conversion. This is one of the most costly process steps. These processes are technically still immature. There are different options for these processes. The enzymatic, microbial processes researched by Dartmouth College are considered to have an outstanding potential.

Biomass waste: a Louisiana rice hulls pile

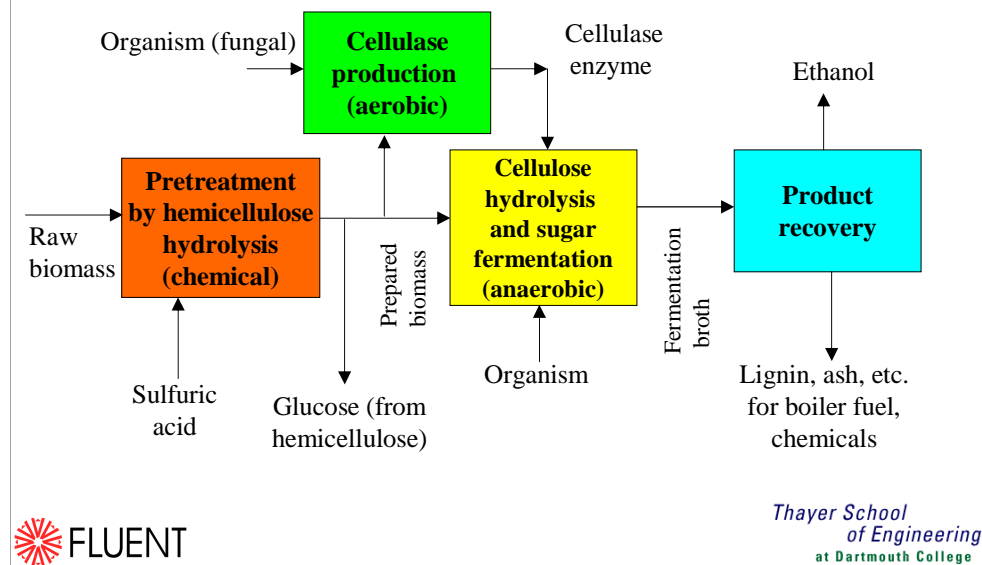


*Thayer School
of Engineering
at Dartmouth College*

Biomass waste is everywhere. An example shown here is a rice hulls pile in Louisiana. When rice gets processed, the brown hulls are removed from the rice, and these are then dumped in landfills. There are many of those landfills throughout rice growing areas in the United States. On the photo can you tell the scale by looking at the trees, and the roads on the pile. You can also see relatively small rectangular dump piles. Each of those is one trailer load full. There are many of such landfills, and all represent usable biomass that is now literally going to waste. Such waste could be put to good use by conversion into ethanol for use as a transportation fuel.

Note: rice hulls can not be burned because they have a high mineral content (which is also what actually makes them healthy to eat). The high mineral content causes slagging and other problems in ovens and burning is not economical. Ethanol is a higher value product than heat from burning and is economically viable.

Enzymatic conversion of biomass to ethanol



Now let's discuss how this process actually works. There are different methods available to carry out the conversion. Here we focus on the enzymatic and microbial conversion process.

(Note: other options are to use chemical hydrolysis, or a full microbial process where the cellulase production step –green box- and the hydrolysis and fermentation –yellow box- are all combined into one microbial process. This is one of Lee's research interests)

We start with the raw biomass. The biomass needs to be pretreated. This is done in a chemical process step. Pretreatment is necessary because the biomass is insoluble and we need to open up the physical structure to make the cellulose accessible to the enzymes used in the later process steps, to ensure a high digestibility. Also in this step, we chemically convert the hemicellulose, which is the easily converted amorphous saccharide, into glucose. The resulting stream is split. The glucose coming from the hemicellulose hydrolysis can be processed separately. The remaining stream is used to feed two other process steps.

One stream is used to feed the cellulase enzyme production step. The cellulase enzyme is produced in a fungal, aerobic fermentation. This is a multiphase fermentation, involving gas-liquid flow. The other stream which contains most of the pretreated biomass is now fed to the main conversion reactor. In this reactor the cellulose hydrolysis and the sugar fermentation take place. This is an anaerobic fermentation, that relies on the cellulase enzymes produced in one of the previous steps.

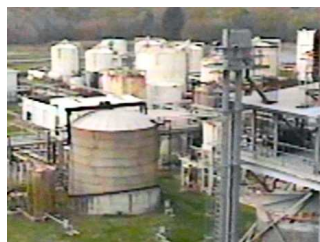
Finally, in the product recovery stage we separate the ethanol product from the waste products. The waste products will include lignin and other materials that can be used as a boiler fuel to provide the energy used in the overall process.

Modeling needs

- Main use of CFD modeling will be in the scale-up from laboratory scale to industrial scale.
- Aerobic fermentation:
 - Multiphase, gas-liquid flow field calculations.
 - Gas-holdup and mass transfer coefficient calculations.
- Anaerobic fermentations:
 - Cellulose hydrolysis, including adsorption, conversion and age distributions.
 - Glucose to ethanol fermentation.



↓ Scale-up



*Thayer School
of Engineering
at Dartmouth College*

Looking at this process, what are the main modeling needs? The main use of the CFD modeling will be in the final scale-up of the small-scale laboratory reactors to the final commercial scale reactors.

Here on the right you see two of my co-authors, Profs. Charlie Wyman and Lee Lynd in their lab. at Dartmouth College. Eventually of course the processes developed there have to be scaled up to the large industrial scale seen on the bottom right.

Of the various process steps, the fermentation steps are the most difficult ones to scale-up. There are two different types of fermentations to be studied. The aerobic fermentation step is used in the cellulase enzyme production. Key design parameters are the gas holdup and mass transfer coefficient. This involves full multiphase, gas-liquid flow field calculations.

The anaerobic fermentations include the enzymatic cellulose hydrolysis and the glucose to ethanol fermentation. Modeling parameters are the adsorption process, the conversion, and age distributions of the various materials, as they affect the final process efficiency.

I will now first briefly speak about the gas-liquid modeling of the aerobic, multiphase fermentation system, and will then speak in more detail about the modeling of the fermentation kinetics.

Aerobic fermenter modeling

- Gas-liquid multiphase flow.
- Full Eulerian multiphase flow modeling:
 - Used to model droplets or bubbles of secondary phase(s) dispersed in continuous fluid phase (primary phase).
 - Allows for mixing and separation of phases.
 - Solves momentum, enthalpy, and continuity equations for each phase and tracks volume fractions.
- Impellers can be modeled transient using the sliding mesh method.
- Key design parameters are gas holdup and mass transfer coefficient $k_L a$.



*Thayer School
of Engineering*
at Dartmouth College

In the aerobic fermenter we encounter a gas-liquid, multiphase flow. We model this using a full Eulerian model. These models are suited to describe the behavior of secondary phases such as droplets and bubbles dispersed in a continuous phase. Eulerian models properly describe both the mixing and separation of phases. They solve the momentum enthalpy, and continuity equations for each phase and track the volume fractions of the various phases. We can combine the Eulerian multiphase models with transient sliding mesh models to describe the impeller motion. Using these models we can then predict the local gas-holdup, bubble size, and $k_L a$.

Volume fraction

- Eulerian multiphase model.
- Volume fraction:

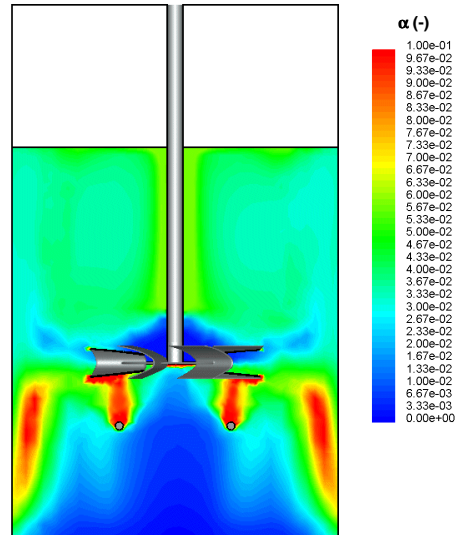
$$\frac{\partial}{\partial t} (\bar{\alpha}_c \rho_c) + \nabla \cdot (\bar{\alpha}_c \rho_c \tilde{U}_c) = S_{\alpha c}$$

- Momentum balance:

$$\frac{\partial}{\partial t} (\bar{\alpha}_c \rho_c \tilde{U}_c) + \nabla \cdot (\bar{\alpha}_c \rho_c \tilde{U}_c \otimes \tilde{U}_c) = -\bar{\alpha}_c \nabla \bar{p} + \nabla \cdot \bar{\tau}_c^t + F_{Dc}$$

- Drag forces:

$$F_{Dc} = K_{dc} \left[(\tilde{U}_d - \tilde{U}_c) - \left(\frac{\alpha_d \bar{u}_d'}{\bar{\alpha}_d} - \frac{\alpha_c \bar{u}_c'}{\bar{\alpha}_c} \right) \right]$$



Thayer School
of Engineering
at Dartmouth College

Using an Eulerian multiphase flow model, we solve a transport equation for the gas fraction. From left to right, the rate of change term plus the convective transport of the phase, equals the phase source term. The tilde over the velocity symbol U indicates a phase-averaged velocity approach.

In the momentum equation, we have from left to right the rate of change plus the convective momentum transport equaling momentum transport due to the pressure forces, shear forces, and momentum exchange terms including the drag force.

The figure shows the local gas-holdup in a 3-D vessel equipped with a radial pumping BT-6 impeller. The two grey circles below the impeller show the cross section of the ring-sparger. This is where the gas enters the vessel. The gas escapes into the open headspace above the liquid surface. The gas holdup in a cross section in between the baffles is shown. The highest gas volume fractions (denoted by the symbol α) are found in the sparger outflow and also near the vessel wall, in the lower circulation loop. In that region the gas and liquid are in counterflow, resulting in higher gas volume fractions.

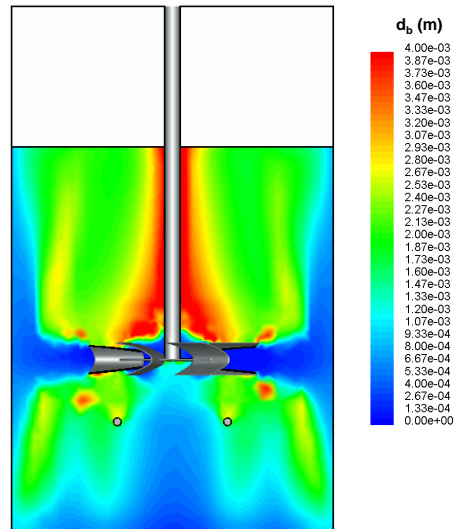
Bubble size

- A single scalar equation is solved for the local bubble number density:

$$\frac{\partial n_b}{\partial t} + \vec{\nabla} \cdot (n_b \vec{u}_g) = S_{bc} + S_{\alpha} / V_{b, in}$$

- This includes coalescence and breakup source terms S_{bc} .
- These include effects of turbulence on the bubble breakup and coalescence behavior.
- Local average bubble size can be calculated from the bubble number density and the volume fraction:

$$n_b = \alpha / V_b$$



 FLUENT

Thayer School
of Engineering
at Dartmouth College

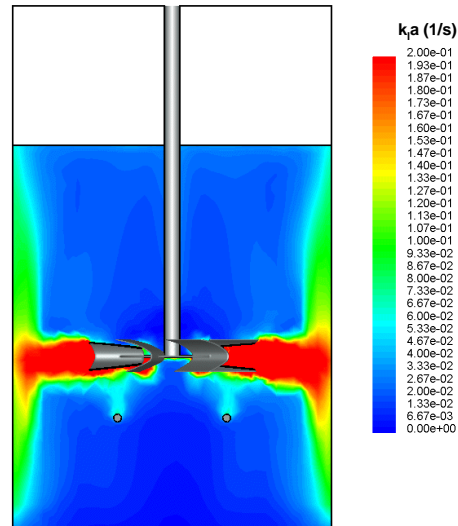
The figure shows the local bubble size in a cross section of the vessel. Bubbles enter the vessel from the sparger at a given size (here ~3mm). They are broken up by the impeller into smaller bubbles (<1mm). These then coalesce into larger bubbles, and the bubble size increases away from the outflow of the impeller. There are red spots near the tips of the impeller blades where bubble size is larger due to the high gas holdup in the vortices shed by the impeller blades.

Mass transfer coefficient $k_L a$

- Interfacial area can be calculated from local gas holdup and bubble size.
- The liquid side mass transfer coefficient k_L is calculated from Kawase and Moo-Young (1990):

$$k_L = 0.301 (\varepsilon \nu)^{1/4} Sc^{-1/2}$$

- Most of the mass transfer will occur in the impeller region, where the turbulence intensity is the highest.



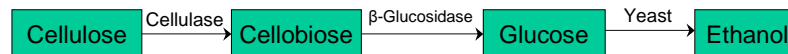
 FLUENT

Thayer School
of Engineering
at Dartmouth College

The figure shows the local mass transfer coefficient $k_L a$ in a cross section of the vessel. $k_L a$ is highest in the impeller region and the impeller outflow, due to the fact that this is where the bubbles are smallest (resulting in a high interfacial area a) and also the liquid side mass transfer coefficient k_L is high due to the high turbulence intensity.

Cellulose conversion

- Multistep process:
 - Enzyme adsorbs to lignocellulose particulates.
 - Enzyme converts cellulose, which is a polysaccharide, to cellobiose, which is a disaccharide.
 - Enzyme converts cellobiose to glucose.
 - Glucose is fermented to ethanol by yeast (*S. Cerevisiae*).



- The last step, glucose to ethanol fermentation by yeast is a well known process.



*Thayer School
of Engineering
at Dartmouth College*

Now, let's look in more detail at the cellulose conversion process. This is a multistep process. First the enzyme adsorbs to insoluble lignocellulose particulates. The enzyme then converts the cellulose, which is a polysaccharide, to cellobiose, which is a disaccharide. A second enzyme then breaks the cellobiose molecules into individual glucose molecules. Glucose is then fermented to ethanol by yeast (*S. Cerevisiae*). This fermentation is well studied and described.

We will first look at the last step, the glucose to ethanol fermentation only. Then we will look at the overall kinetics including the adsorption and hydrolysis steps.

Kinetic model for glucose fermentation

- Model was adapted from Krishnan et al. (1999):

$$\text{Cells: } r_x = \frac{Xc \times \mu_{\max} \times G}{K_G + G + \frac{G^2}{K_{GI}}} \times \left\{ 1 - \left(\frac{P}{K_{X/P}} \right)^\beta \right\} \times \frac{[A]}{[A] + K_A}$$

$$\text{Ethanol: } r_p = \frac{Xc \times v_{\max} \times G}{K_G + G + \frac{G^2}{K_{GI}}} \times \left\{ 1 - \left(\frac{P}{K_{X/P}} \right)^\gamma \right\} \times \frac{[A]}{[A] + K_A}$$

$$\text{Glucose: } r_G = \frac{-r_x}{Y_{X/G}} + m \times X$$

$$\text{Ammonia: } r_A = r_G Y_{NG}$$



Thayer School
of Engineering
at Dartmouth College

There are many different models available for the glucose to ethanol fermentation by yeast, including simple Monod kinetics. The models we use are slightly modified versions of models presented in the literature by Krishnan et al. These models are suitable for the full range of cell and substrate concentrations. (Monod kinetics only works for lower glucose concentrations, <40 g/L initial glucose in batch systems). We have a rate of cell growth equation that includes both product inhibition terms and a term involving the availability of Ammonia (which is a necessary chemical to provide nitrogen to the cells).

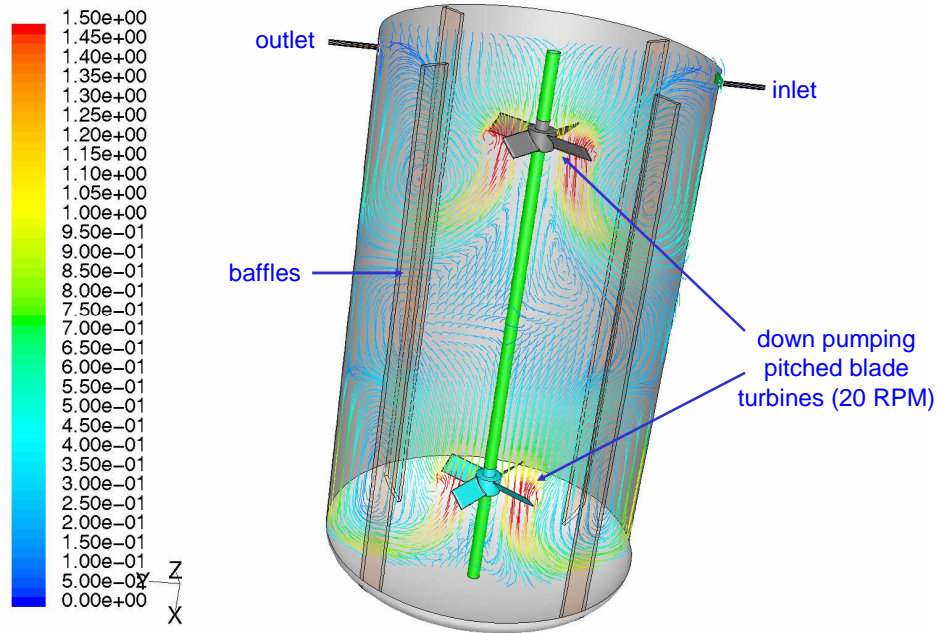
μ = specific growth rate of cells (g cells/g cells hr)

μ_{\max} = maximum specific growth rate (hr^{-1})

K_G = saturation constant (g/L)

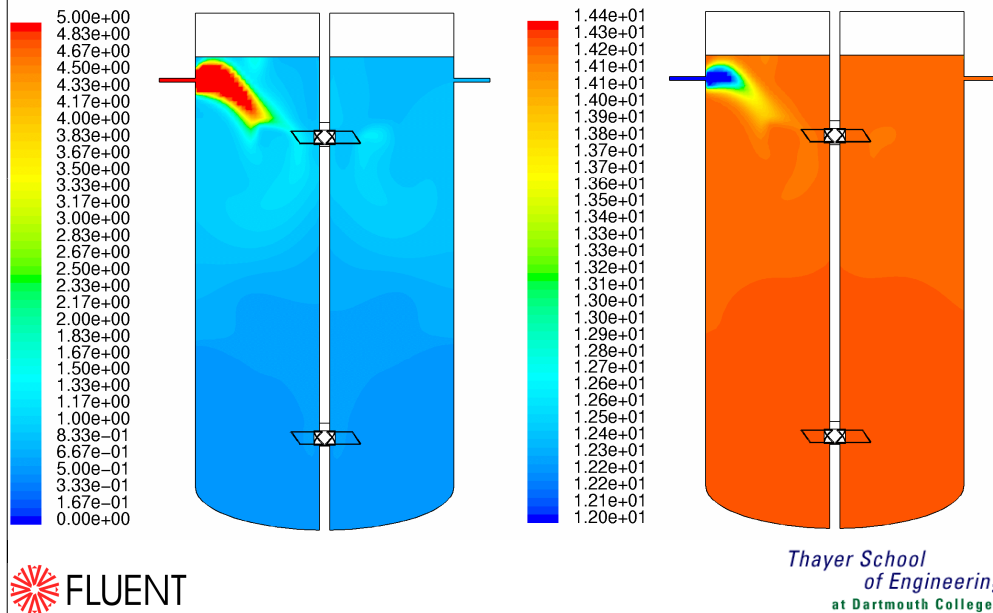
[G] = concentration of the glucose – the rate limiting substrate (g/L)

Large scale fermenter



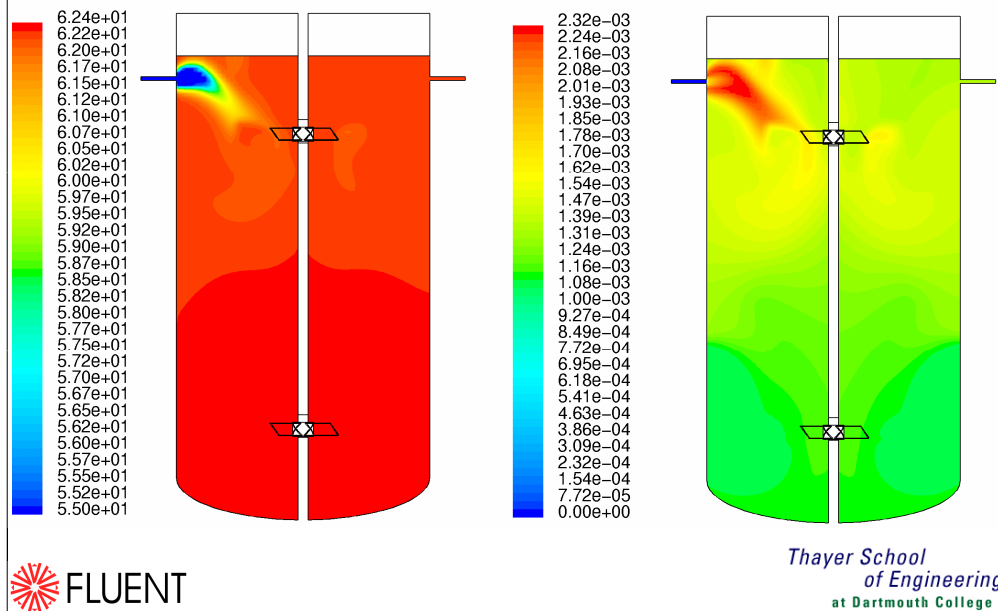
As a calculation example we can look at a 500,000 gallon, or 1900 m³ fermenter. The vessel diameter is 10.8 m. This fermenter is equipped with two down pumping pitched blade turbines. There is a side inlet, and a side outlet. The residence time in the vessel is 18 hours. Two main circulation loops form. The colors indicate the local velocity magnitude in m/s. This simulation is performed using a multiple reference frame (MRF) model for the impellers.

Final glucose and cell concentration



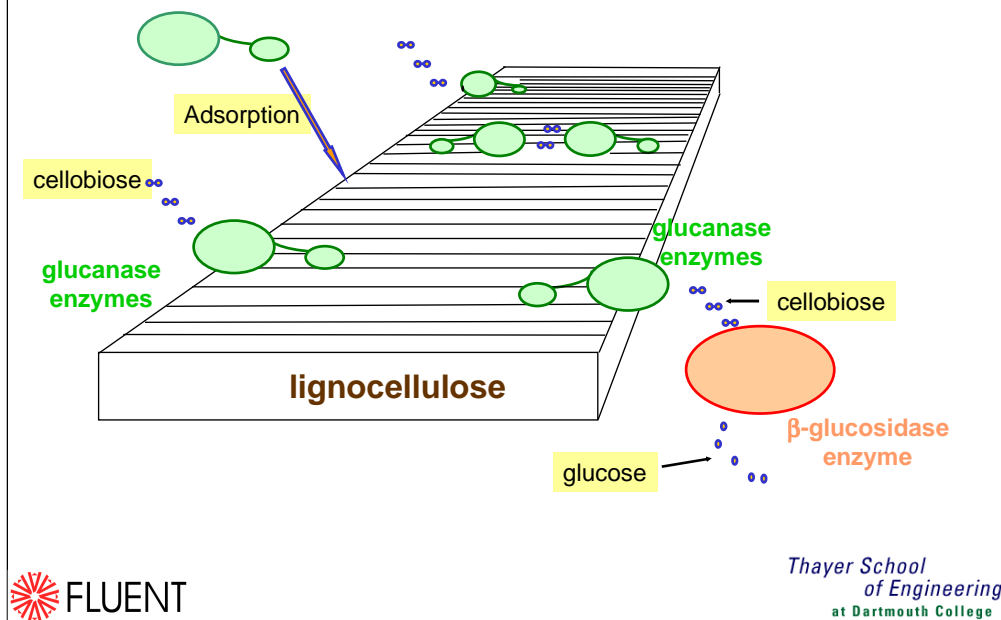
Here we see the final glucose (left) and cell concentrations (right). The concentrations are in g/L. A plume forms at the inlet, with locally high glucose and low cell concentrations.

Ethanol concentration and production rate



We see similar plumes form for the ethanol concentration (left) and the ethanol production rate (right). Concentration is in g/L and production rate in g/L/s. You can see that there is at least a factor of two difference in the ethanol production rate in the vessel.

The enzymatic cellulose hydrolysis step



Now that we looked at the glucose to ethanol fermentation step, let's look at the step before that; which is the hydrolysis, the conversion of the cellulose to glucose.

It is important to realize that we are working with an insoluble medium. And the first step in the hydrolysis is in fact an adsorption step; the attachment of the enzymes to the surface of the substrate. The substrate mainly consists of lignin and cellulose. The hemicellulose present in the raw biomass has been removed in the pretreatment step. Two main enzymes are present. The glucanase enzymes adsorb ("attach") to the surface of the substrate. They then convert the cellulose polymers to a material called cellobiose. Cellobiose consists of two glucose molecules attached to each other by a chemical bond. The cellobiose is then broken into individual glucose molecules by a second enzyme, called beta-glucosidase. This enzyme is not adsorbed to the substrate surface, but floats around freely through the liquid.

Effects of age and conversion

- Reactivity of the lignocellulose particles and the cellulose-enzyme complex decrease with increasing conversion and age.
- The exact cause of this is not fully understood, but is assumed to be largely due to mechanical/physical phenomena, and not due to chemical effects.
- Experience has shown that the effects of age and conversion have to be taken into account in any mathematical model, in order to obtain quantitatively accurate results.
- The CFD model developed for this uses a population balance approach for lignocellulose substrate and cellulose-enzyme complex of different ages.



*Thayer School
of Engineering*
at Dartmouth College

It is known that the reactivity of the lignocellulose particles and the cellulose-enzyme complex decrease with increasing conversion and age.

The exact cause of this is not fully understood, but is assumed to be largely due to mechanical/physical phenomena, and not due to chemical effects.

Experience has shown that the effects of age and conversion have to be taken into account in any mathematical model, in order to obtain quantitatively accurate results.

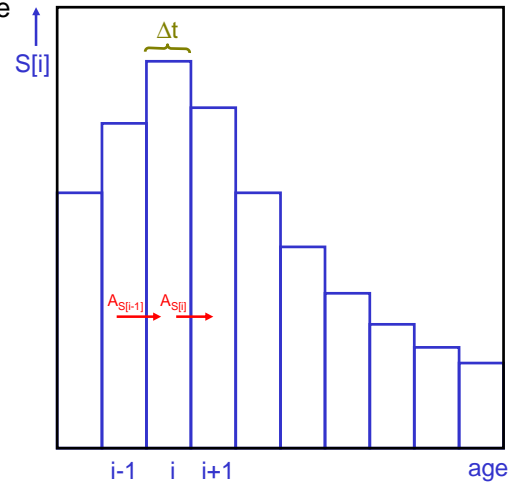
The CFD model developed for this uses a population balance approach for lignocellulose substrate and cellulose-enzyme complex of different ages.

Age distribution modeling

- $S[i]$ and $CE1[i]$ are concentrations of species S and CE1 with an age between $(i-1/2)\Delta t$ and $(i+1/2)\Delta t$
- For each species, aging source terms are added to the transport equations, which then become:

$$\frac{\partial S(i)}{\partial t} + \vec{u} \cdot \vec{\nabla} S(i) = \vec{\nabla} \cdot (D_t \vec{\nabla} S(i)) + r_{S(i)} + A_{S(i-1)} - A_{S(i)}$$

rate of change \downarrow $\frac{\partial S(i)}{\partial t}$
 convection \downarrow $\vec{u} \cdot \vec{\nabla} S(i)$
 diffusion \downarrow $\vec{\nabla} \cdot (D_t \vec{\nabla} S(i))$
 reaction or adsorption \nearrow $r_{S(i)}$
 aging of S(i-1) \nearrow $A_{S(i-1)}$
 aging of S(i) \nearrow $-A_{S(i)}$



Thayer School
of Engineering
at Dartmouth College

When modeling this process we therefore have to include the effect of age and conversion on the reactivity. This is done by calculating an age distribution for the individual affected species. The two main species where this applies to, are the lignocellulosic substrate and the cellulose-enzyme complexes. For each of those we keep track of ten subspecies of different age, to calculate an age distribution. We can do this by solving transport equations for these species as before, including the rate of change, the convective and diffusive transport, the reaction or adsorption source term, and aging source terms. The final result is that for each of these species we will know the age distribution. This allows us to calculate the conversion for species of different age, and hence to include the effect of declining reactivity with increasing time and conversion into the model.

Cellulose kinetic model with age distribution

$$\begin{aligned}
 \text{Rate of enzyme} \quad r_{E1} &= -\sum_{i=1}^n \frac{0.0806}{\sigma_S} r_{CE1(i)} - \frac{0.0123}{\sigma_L} r_{LE1} & \text{Rate of lignin} \quad r_L &= -\frac{1}{\sigma_L} \times r_{LE1} \\
 \text{Cellulose-enzyme ads.} \quad r_{CE1(i)} &= -(k \times (1 - x_{p(i)})^m + c) \times [CE1(i)] \times \frac{K_{S/C}}{[CB] + K_{S/C}} \times \frac{K_{S/P}}{[P] + K_{S/P}} + 2 \times (k_{f1} \times [E1] \times \sigma_S \times [S(i)] - k_{r1} \times [CE1(i)]) \\
 \text{Lignin-enzyme ads.} \quad r_{LE1} &= k_{f2} \times [E] \times \sigma_L \times [L] - k_{r2} \times [LE1] \\
 \text{Rate of cellulose reaction} \quad r_{S(i)} &= -(k \times (1 - x_{p(i)})^m + c) \times \frac{[CE1(i)]}{\sigma_S} \times \frac{K_{S/C}}{[CB] + K_{S/C}} \times \frac{K_{S/P}}{[P] + K_{S/P}} - \frac{1}{\sigma_S} \times r_{CE1(i)} \\
 \text{Rate of cellobiose reaction} \quad r_{CB} &= -1.056 \times \sum_{i=1}^n (r_{S(i)} + \frac{1}{\sigma_S} \times r_{CE1(i)}) - \frac{K_C \times [CB] \times [E2]}{K_m \times (1 + \frac{[G]}{K_{C/G}}) + [CB]} \\
 \text{Rate of cell growth} \quad r_{Xc} &= \frac{[X_C] \times \mu_{\max} \times [G]}{[G] + K_G} \times (1 - \frac{[P]}{K_{X/P}}) & \text{Rate of CO}_2 \text{ prod.} \quad r_{CD} &= r_P \times \frac{22}{23} \\
 \text{Rate of glucose reaction} \quad r_G &= (-1.056 \times \sum_{i=1}^n (r_{S(i)} + \frac{1}{\sigma_S} \times r_{CE1(i)}) - r_{CB}) \times 1.053 - \frac{r_{Xc}}{Y_{X/G}} \\
 \text{Rate of ethanol prod.} \quad r_P &= r_{Xc} \times \frac{Y_{P/G}}{Y_{X/G}} & \text{Conversion} \quad x_i &= 0.97 - \frac{[S(i)]}{[S_0(i)]} \\
 \text{Substrate conservation} \quad [S_i(i)] &= [S(i)] + \frac{[CE1(i)]}{\sigma_S}
 \end{aligned}$$



Thayer School
of Engineering
at Dartmouth College

Here we see the full set of kinetic equations for the adsorption, hydrolysis, and fermentation process.

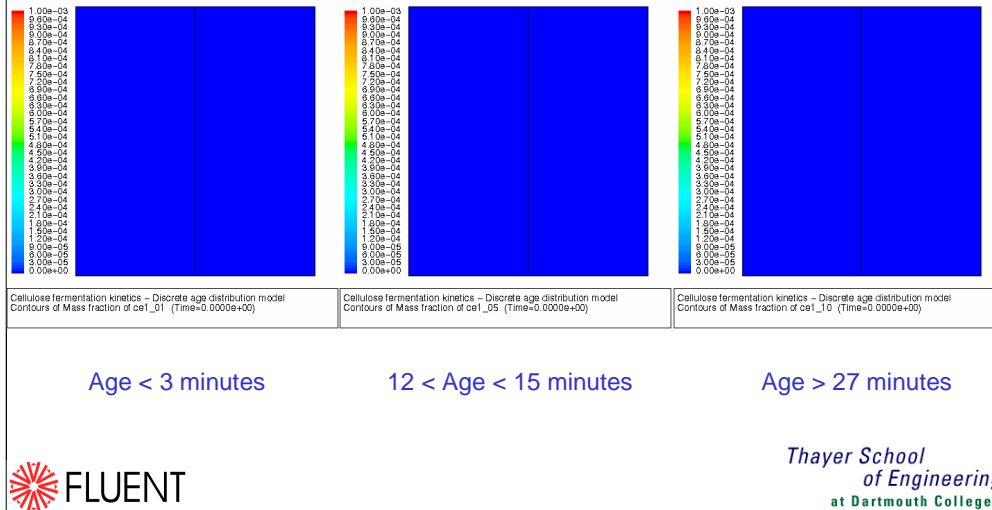
The model includes several important effects:

- Rate saturation with respect to either substrate or enzyme based, on adsorption,
- Declining reaction rate with conversion using an age distribution model.

These features deviate from classical kinetics for soluble substrates.

Mass fraction of cellulose-enzyme complex

- The mass fraction of the cellulose-enzyme complex CE1 of three different ages at time 0 s.



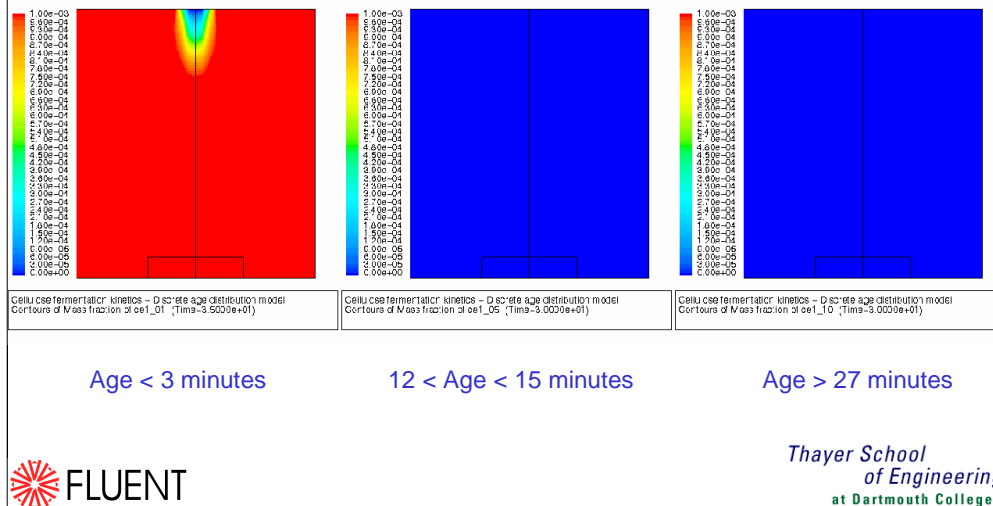
These pictures are for a 0.75 L beaker with no baffles and a magnetic stirrer at ~150 RPM.

Material enters in the center top of the beaker, and exits on the side, just above the stirrer. These are 2-D axisymmetric models with swirl. The stirrer was modeled by prescribing a tangential source term in the stirrer region.

The pictures show the mass fractions of three of the ages of cellulose-enzyme complexes. We can see how the concentrations increase with time, how the concentrations of the older ages are lower, and obviously start to form at a later time.

Mass fraction of cellulose-enzyme complex

- The mass fraction of the cellulose-enzyme complex CE1 of three different ages at time ~30 s.



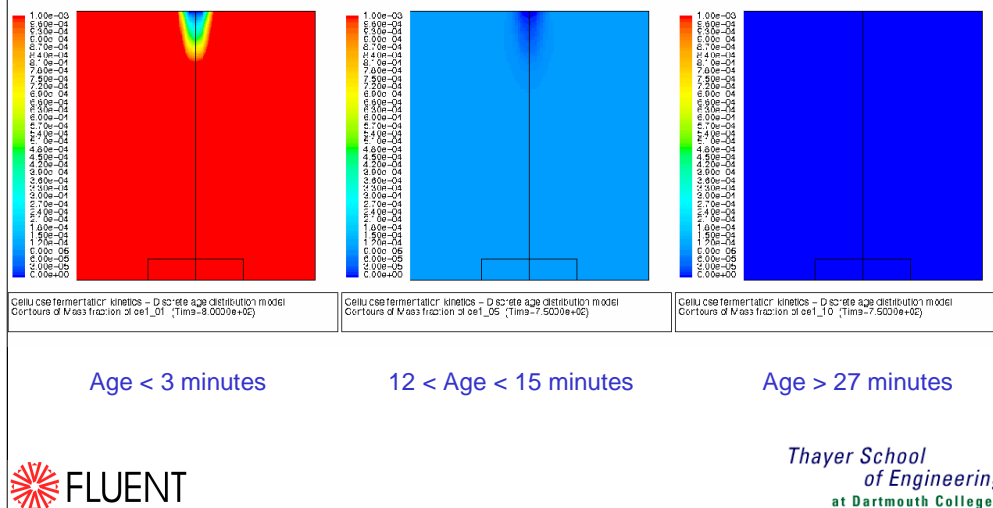
These pictures are for a 0.75 L beaker with no baffles and a magnetic stirrer at ~150 RPM.

Material enters in the center top of the beaker, and exits on the side, just above the stirrer. These are 2-D axisymmetric models with swirl. The stirrer was modeled by prescribing a tangential source term in the stirrer region.

The pictures show the mass fractions of three of the ages of cellulose-enzyme complexes. We can see how the concentrations increase with time, how the concentrations of the older ages are lower, and obviously start to form at a later time.

Mass fraction of cellulose-enzyme complex

- The mass fraction of the cellulose-enzyme complex CE1 of three different ages at time ~750 s.



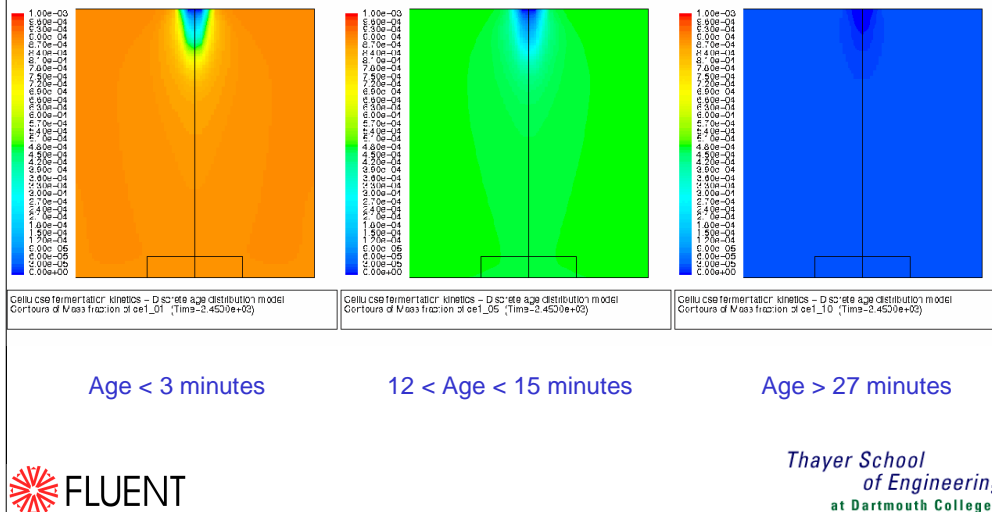
These pictures are for a 0.75 L beaker with no baffles and a magnetic stirrer at ~150 RPM.

Material enters in the center top of the beaker, and exits on the side, just above the stirrer. These are 2-D axisymmetric models with swirl. The stirrer was modeled by prescribing a tangential source term in the stirrer region.

The pictures show the mass fractions of three of the ages of cellulose-enzyme complexes. We can see how the concentrations increase with time, how the concentrations of the older ages are lower, and obviously start to form at a later time.

Mass fraction of cellulose-enzyme complex

- The mass fraction of the cellulose-enzyme complex CE1 of three different ages at time ~2450 s.



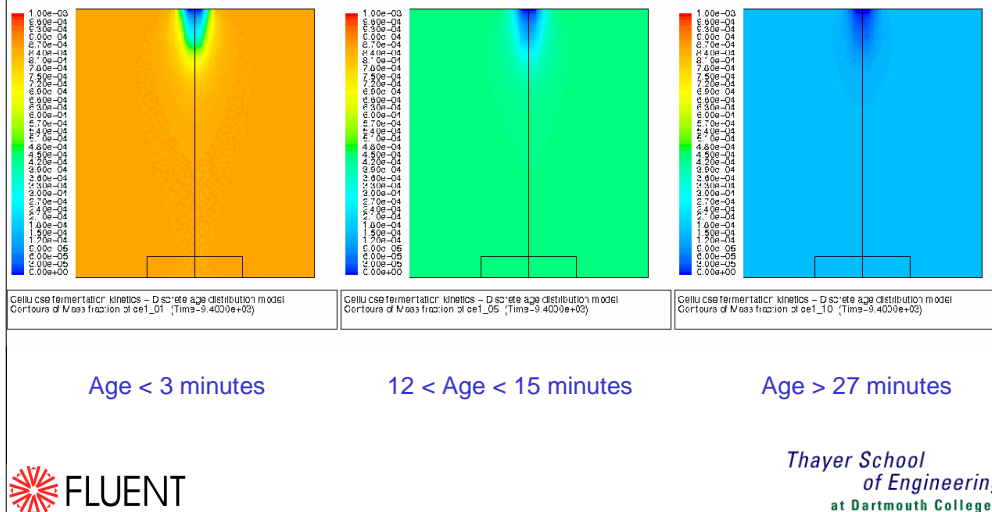
These pictures are for a 0.75 L beaker with no baffles and a magnetic stirrer at ~150 RPM.

Material enters in the center top of the beaker, and exits on the side, just above the stirrer. These are 2-D axisymmetric models with swirl. The stirrer was modeled by prescribing a tangential source term in the stirrer region.

The pictures show the mass fractions of three of the ages of cellulose-enzyme complexes. We can see how the concentrations increase with time, how the concentrations of the older ages are lower, and obviously start to form at a later time.

Mass fraction of cellulose-enzyme complex

- The mass fraction of the cellulose-enzyme complex CE1 of three different ages at time ~9400 s.

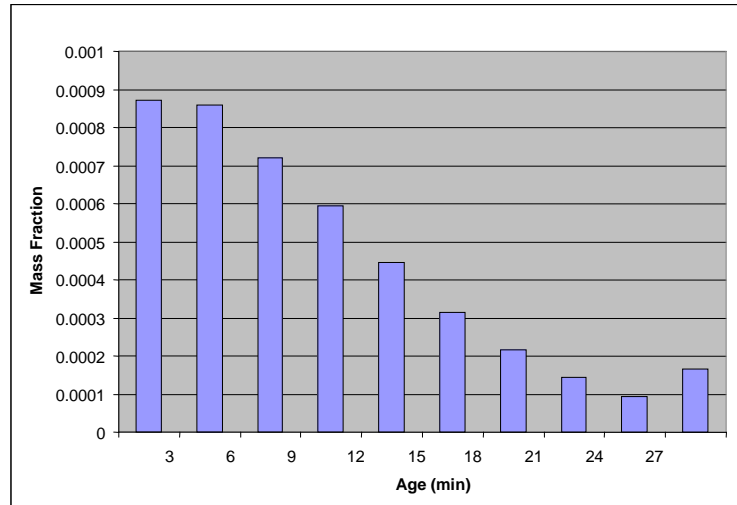


These pictures are for a 0.75 L beaker with no baffles and a magnetic stirrer at ~150 RPM.

Material enters in the center top of the beaker, and exits on the side, just above the stirrer. These are 2-D axisymmetric models with swirl. The stirrer was modeled by prescribing a tangential source term in the stirrer region.

The pictures show the mass fractions of three of the ages of cellulose-enzyme complexes. We can see how the concentrations increase with time, how the concentrations of the older ages are lower, and obviously start to form at a later time.

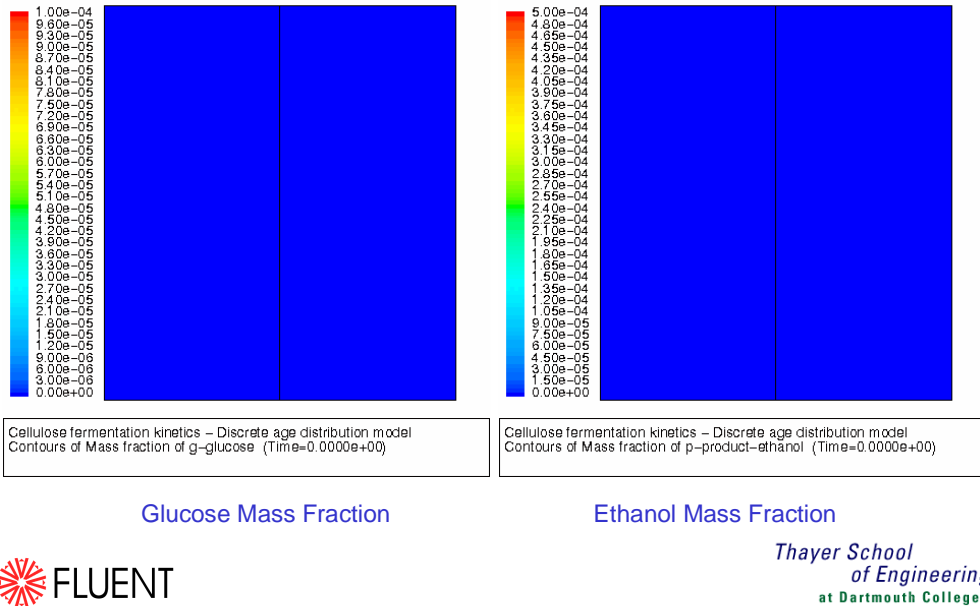
Cellulose-enzyme complex age distribution



Thayer School
of Engineering
at Dartmouth College

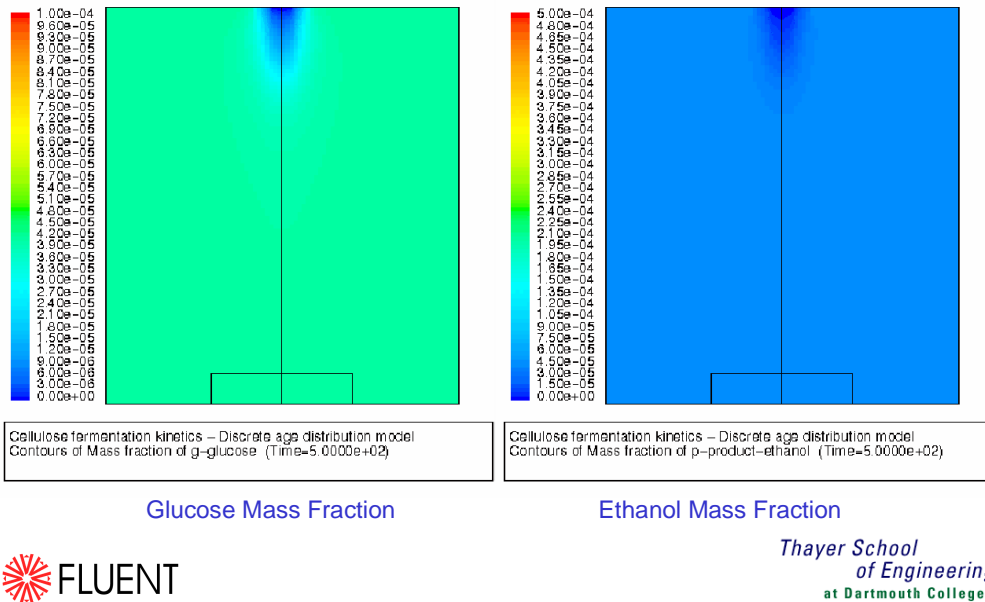
From that we can calculate age distributions, as shown in this histogram, showing the relative mass fractions of species of different ages.

Glucose and ethanol (Time = 0s)



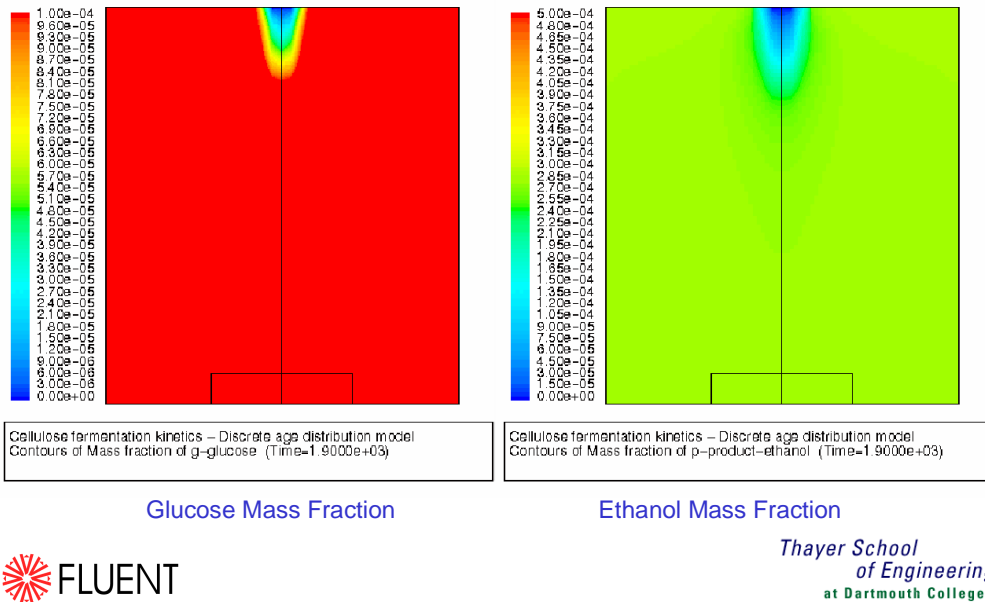
These pictures show the glucose and ethanol mass fractions in the same beerglass. Note that the color scale is different, and the ethanol mass fraction is actually higher than the glucose fraction.

Glucose and ethanol (Time = 500s)



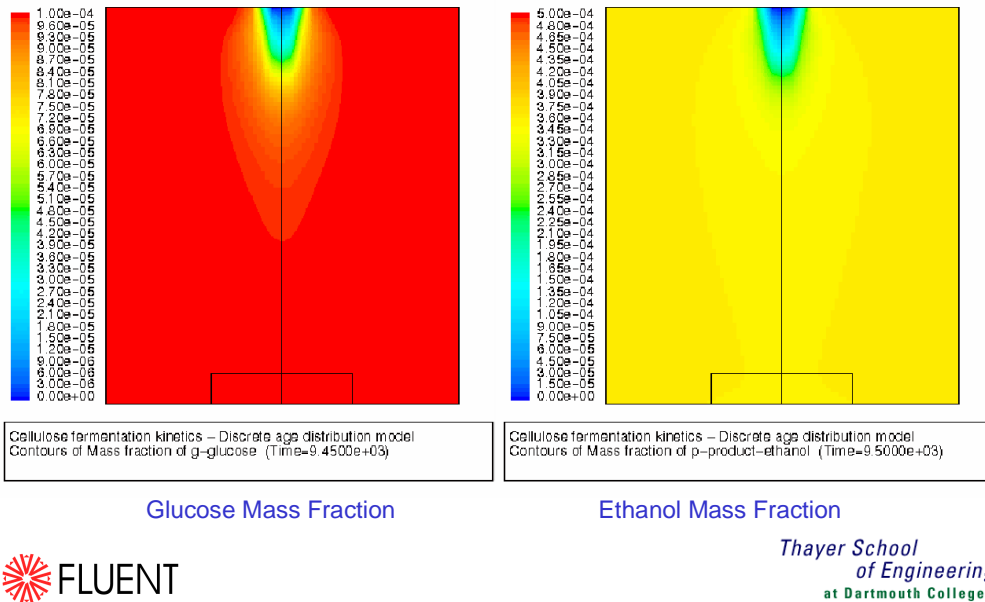
These pictures show the glucose and ethanol mass fractions in the same beaker. Note that the color scale is different, and the ethanol mass fraction is actually higher than the glucose fraction.

Glucose and ethanol (Time = 1900s)



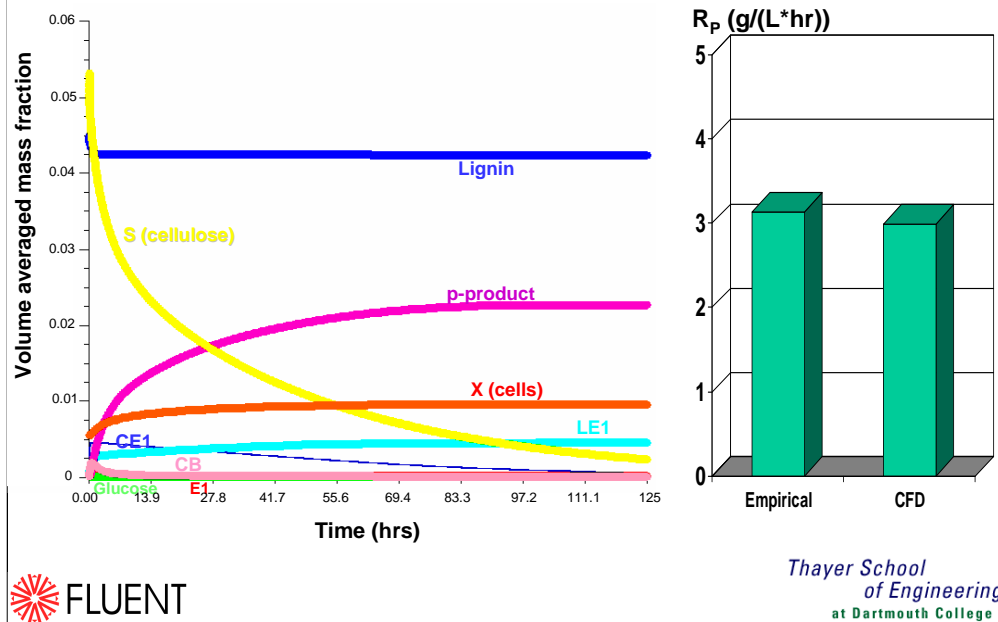
These pictures show the glucose and ethanol mass fractions in the same beaker. Note that the color scale is different, and the ethanol mass fraction is actually higher than the glucose fraction.

Glucose and ethanol (Time = 9500s)



These pictures show the glucose and ethanol mass fractions in the same beaker. Note that the color scale is different, and the ethanol mass fraction is actually higher than the glucose fraction.

Typical simulation results



Here we show some typical quantitative simulation results. The x-y graph shows concentration curves for different species for a batch model using batch kinetics for the insoluble lignocellulosic substrate (for a beakerglass). The bar chart shows values for averaged ethanol productivity R_p (g/L*hr) also for a beakerglass; but now for a soluble glucose substrate simulation (comparing CFD results with results of an empirical model).

Some general issues

- Tens of model constants and tens of scalar equations:
 - Lignocellulose particles (10 eqns.).
 - Cellulose-enzyme complex. (10 eqns.).
 - Conversion rate (10 eqns.).
 - Cells.
 - Ethanol.
 - Glucose.
 - Ammonia.
 - Lignin.
 - Enzymes (2 eqns.).
 - Lignin-enzyme complex
 - Cellobiose.
 - CO₂.
- Model complexity and large numbers of constants require significant model tuning to ensure valid results.



*Thayer School
of Engineering*
at Dartmouth College

Model complexity and large numbers of constants require significant model tuning to ensure valid results.

Conclusions

- Cellulosic biomass to ethanol conversion is an important technology to meet future fuel demands.
- A full model for the combined adsorption, hydrolysis, and fermentation of pretreated lignocellulose has been developed.
- The effect of age distributions has been implemented by means of a population balance approach.
- CFD simulations agree well with empirical model results.
- It seems that fed-batch reactors will be more efficient than batch or continuous flow reactors.
- Continued development and application of combined kinetic and CFD models is underway



*Thayer School
of Engineering*
at Dartmouth College

Prof. Wyman recently (2004) published a very nice article titled “Ethanol Fuel” in the Encyclopedia of Energy.